JOURNAL OF MATERIALS SCIENCE 19 (1984) 1863–1875

Effect of temperature on deformation and fracture of notched polymers

M. KITAGAWA, H. YAMMAURA
Department of Mechanical Engineering, Faculty of Technology, Kanazawa University, Kanazawa, Japan

The fracture processes in notched polycarbonate (PC) and polypropylene (PP) bars subjected to 3-point bending have been investigated in the wide range from liquid nitrogen to glass transition temperatures. There exist several temperature regions which distinguish the fracture mechanism. For PC, the brittle fracture was preferentially governed by slip or shear bands at relatively high temperatures, but by crazes at low temperatures. For PP, on the other hand, crazing plays an important roll in the fracture over the entire temperature ranges tested. A slip line field analysis, which takes into account the effect of the hydrostatic stress component on the yield criterion, is executed to explain the shape of the plastically deformed region at general yielding and a criterion on the initiation of the slip-inducing fracture. The slip line field analysis is shown to be successfully applied even to a soft material with low elastic modulus like polymer.

1. Introduction

Studies on strength and fracture of polymer solids have been recently investigated especially in the field of crack growth due to fatigue or creep. However, little attention has been paid to the notch brittle fracture, while it is one of the fundamental problems of polymer fracture.

According to the previous papers [1, 2], brittle fracture occurs as follows: When the applied load exceeds a certain level, shear or slip bands initiate at the notch root. Being developed by further loading, they become curved and the form of a logarithmic spiral becomes evident. The extension of the plastic zone including slip bands increases the stress at the elastic–plastic boundary due to the plastic constraint to initiate a crack-like flaw, i.e. a fracture nucleus. The nucleus propagates in a brittle manner to lead to a final fracture. In other words, the fracture process passes through three stages as follows: (a) initiation and extension of shear bands from the notch, (b) nucleation and slow growth of the fracture nucleus at the elastic–plastic interface and (c) rapid propagation of the nucleus. This process is very similar to that of mild steel in the temperature region III defined by Tetelman and McEvily [3].

However, since the previous experiments [1, 2] were performed only in the narrow temperature ranges near room temperature, it remains vague whether or not the process mentioned above covers the mechanism of polymer brittle fracture over wide temperature ranges. Furthermore, the above process may not always be valid for other polymers including crystalline ones.

The purpose of this paper, therefore, is to provide the experimental data of the mechanism of brittle fracture in wide ranges of temperature from liquid nitrogen to glass transition temperature using crystalline and amorphous polymers, and to describe a criterion for the nucleus initiation. Then, the slip line field analysis, which takes into account the effect of hydrostatic pressure on the yeild condition, is used to infer the stress distribution in the plastically deformed region.

2. Experimental procedure

The materials used were commercial polycarbonate (PC), poly(vinyl chloride) (PVC) and polypropylene (PP) plates 10 mm thick (Takiron Co. Japan). Test pieces, the dimensions of which are shown in Fig. 1, were machined from these plates. Unnotched specimens 8 mm high were also pre-

0022–2461/84 $03.00 + .12 © *1984 Chapman and Hall Ltd.*

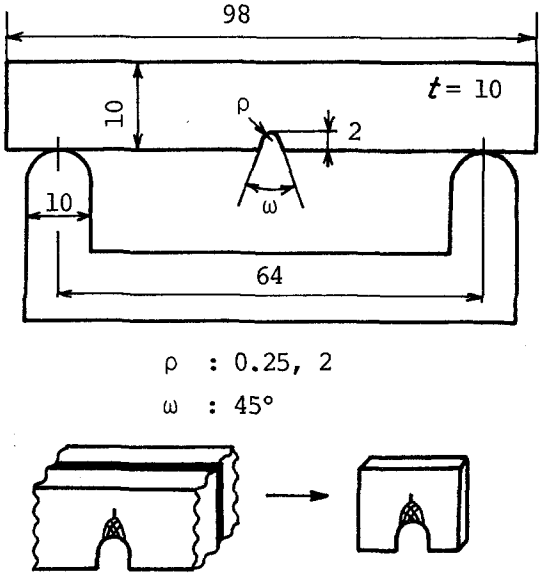

Figure 1 Schematic illustration of test specimen and thin slice for observation.

pared. All specimens were annealed for 2 h at 155° C for PC, at 85° C for PVC and 110° C for PP, and slowly cooled down to room temperature in an electric oven.

Three-point bending tests were performed at a constant crosshead speed of 0.6 mm min^{-1} in the temperature ranges −197 to 150° C. At temperatures lower than room temperature, liquid nitrogen and dry ice were used as cooling agents. To prevent the effect of the cooling agent on brittle fracture, a cooling chamber was devised so that the test specimen was not in direct contact with the environmental agent. However, the specimen was not completely veiled in the evaporated gas. For the tests at −197° C, the specimens were immersed in liquid nitrogen. The cooling agents used are known to act as crazing agents. In order to investigate the effect of the cooling agents on the fracture load, some specimens, the notch parts of which were thinly or thickly covered by a binding agent, were subjected to bending. However, the results at −197° C were not very different from the data of that obtained for the specimens. At temperatures higher than room temperature, an electric heater was used. The fluctuation of the temperature during the test, which was measured by a thermocouple, was within ± 3° C for all temperature ranges tested.

The specimen size and the bending velocity are slightly different from the previous ones [2]. These slight differences may not be of importance for investigating the mechanism of the polymer brittle fracture.

Besides the above experiment, the effect of the notch root radius on the position of the fracture origin was investigated at room temperature using PC and PVC samples. Four-point bending and tensile specimens were also prepared for this test.

Microscopic observations were made on specimens unloaded during deformation and after fracture. As illustrated in Fig. 1, thin slices were cut in order to observe the extension of deformation bands from the notch tip and the initiation of fracture nuclei.

3. Slip line field analysis

A slip line field solution for a round notched bar of a pressure dependent yield material is slightly different from the well-known solution given by Hill. In a plane strain state, the stresses in the plastic region surrounded by a pair of logarithmic spirals are described by

$$\sigma_\theta = \left[1 - \frac{1-\sin\Phi}{1+\sin\Phi}\left(\frac{r}{\rho}\right)^\xi\right] C\cot\Phi$$

$$\sigma_r = \left[1 - \left(\frac{r}{\rho}\right)^\xi\right] C\cot\Phi$$

$$\sigma_m = \left[1 - \frac{\sin^2\Phi/3+1}{\sin\Phi+1}\left(\frac{r}{\rho}\right)^\xi\right] C\cot\Phi$$

$$\xi = -2\sin\Phi/(1+\sin\Phi) \qquad (1)$$

where r and θ are polar coordinates, σ_m is the hydrostatic stress component and C and Φ are the materials constants. The value of $\pi/2 - \Phi$ denotes the acute angle of the intersection between the slip lines. When $\Phi = 0$, Equation 1 reduces to the well-known solution for a pressure-independent yield material. The details of the method for obtaining Equation 1 are described in the previous paper [2].

In this paper, we consider the slip line field at general yielding. The slip line patterns are shown in Fig. 2. The fields consist of a logarithmic spiral region at the notch side, a straight line region at the flat surface and circular arcs which combines both regions. The slip lines at the notch side and at the flat surface are determined by the stress-free boundary. For a pressure dependent yield material with $\Phi \neq 0$, the arc PQ becomes a logarithmic spiral which corresponds to the circular arc for a $\Phi = 0$ material [4]. The six unknown parameters included in Fig. 2 are calculated by the geometric conditions of the specimen, the modified Hencky's theorem [5] and the equilibrium of the forces

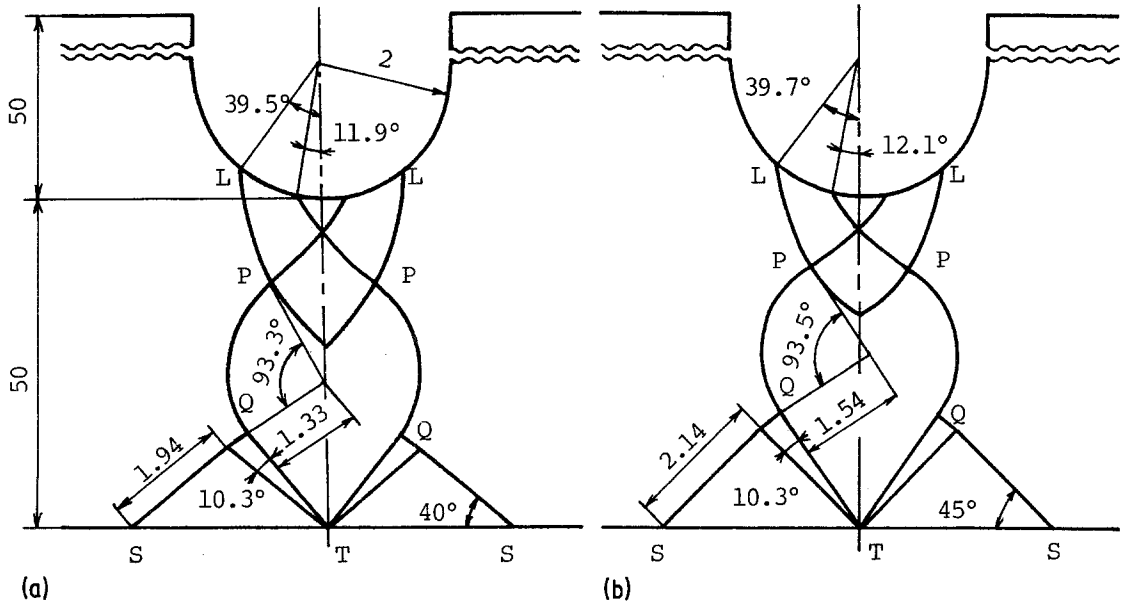

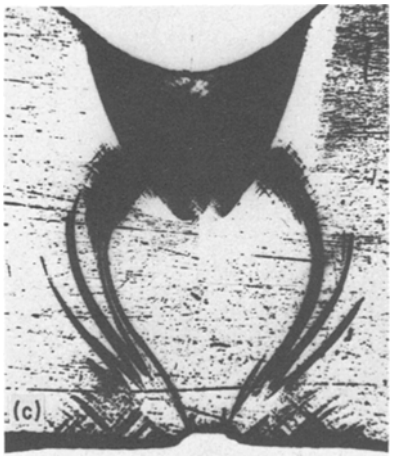

Figure 2 Theoretical and experimental slip line fields at general yielding due to 3-point bending: (a) theoretical ($\Phi = 10°$); (b) theoretical ($\Phi = 0°$); (c) experimental (PC).

along the outer slip lines. The values of the parameters calculated in this way are shown for both cases of $\Phi = 0$ and 10° in Fig. 2. The theoretical fields are very similar to the experimental one indicated in Fig. 2c. The plastic constraint factors for the specimen dimension shown in Fig. 2 are 1.187 for $\phi = 0°$ and 1.185 for $\Phi = 10°$, which are slightly different from the experimental value of 1.26.

The theoretical fields with various notch dimensions can be calculated in the same way. But the corresponding experimental-patterns could not be obtained since fracture occurred before general yielding.

The good agreement between the theoretical and the experimental slip line fields may provide evidence that the slip line field analysis may become a useful approach even for soft materials such as polymers with relatively low elastic moduli.

4. Fracture at room temperature

The fracture process for PP is shown in Fig. 3, which should be compared with the previous result of PC (see Fig. 7 in [2]). It is to be noted that the fracture process of PP is slightly different from that of PC. The brittle fracture process of PC passes through three stages as mentioned in Section 1. On the other hand, for PP, the deformation bands propagate along the radial direction of the round notch, and some of the bands coalesce and become intense with increasing applied load. These bands are considered crazes because of their growth direction which is probably normal to the maximum principal stress. The region including numerous radial lines is shaped like a curved triangle which resembles the plastic zone for PC. Although shear bands may form in this region, they are not observed because of the opaqueness of PP. The fracture seems to occur within one of the intense craze bands away from the notch root, but not at the elastic–plastic boundary. When the fracture nucleus initiates, large plastic deformation occurs at the notch root. The orientation of poly-

mer chains due to this deformation may raise the fracture strength of PP and therefore, may reinforce the material at the notch side. Consequently, the position of the nucleus is influenced by the degree of the notch root elongation. At relatively high temperatures where the notch root elongation is large, the position of the nucleus may become distant from the notch root.

The above discussions show that the fracture mechanism at room temperature is somewhat different between crystalline and amorphous polymers. The fracture of PP is mainly governed by the initiation and coalescence of crazes, whereas for PC, it occurs due to the plastic constraint of the shear bands. Hereafter, the former is called craze-inducing fracture, and the latter slip-inducing fracture.

5. Effect of temperature on fracture process

Fig. 4 denotes the load–deflection curves at various temperatures in PC samples with $\rho =$ 2 mm. It was found that the trends of the curves at -197°C, -140°C and -110 to 80°C are different from each other. In the temperature ranges -110 to 80°C, both load and displacement at fracture monotonically increased with decreasing temperature. At -140°C, the fracture displacement was smaller than that at -110°C. There seems to exist a transition temperature concerning the fracture behaviour.

Fig. 5 shows the variation of fracture or general yield load with temperature for specimens with different notch radii. Also included in the figure are the results for unnotched samples. Irrespective of the specimen geometry, the trends are very similar to each other. It is found that some distinctive regions exist as divided in the figure. The transition temperature from one region to the other is slightly dependent on the notch radius. Then, the fracture process mentioned in Section 4 and the previous paper [2] may provide only one mechanism among these regions and, therefore, is not always valid over the entire temperature regions tested.

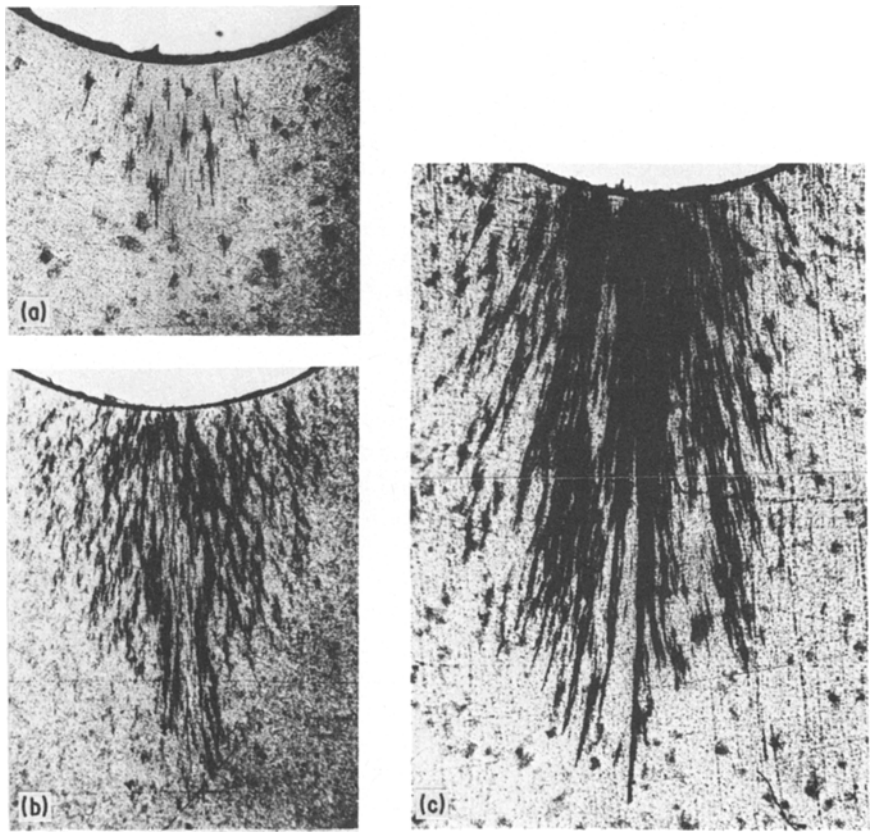

Figure 3 Fracture processes at room temperature for PP specimens with $\rho = 2$ mm. P and P_y are the applied load for notched specimen and the yield load for unnotched specimen. (a) $P/P_y = 0.8$, (b) $P/P_y = 0.92$, (c) $P/P_y = 1.02$.

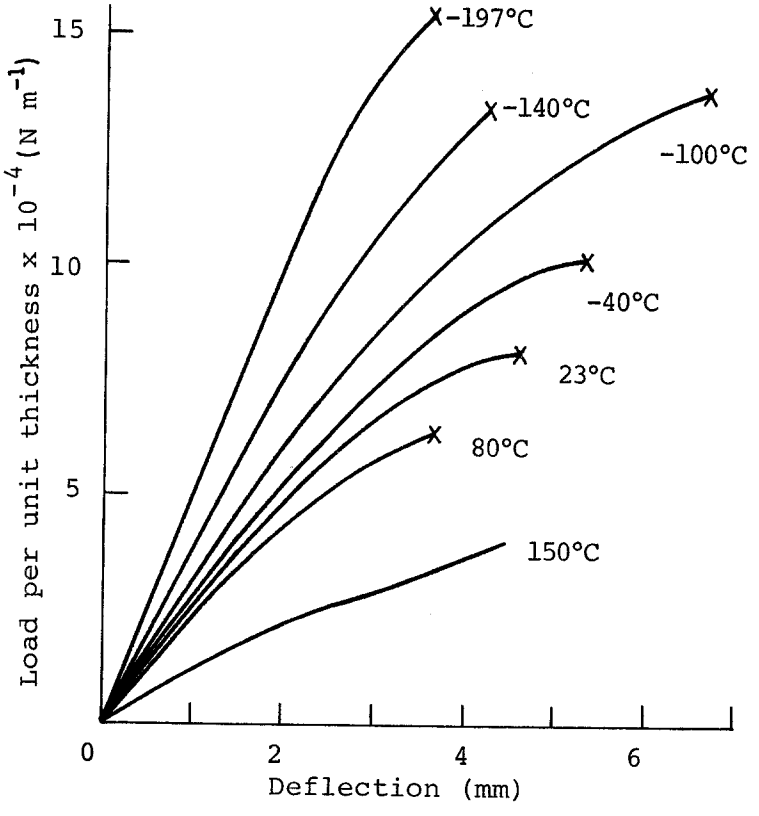

Figure 4 Load–deflection curves at different temperatures for PC specimens with $\rho = 2$ mm.

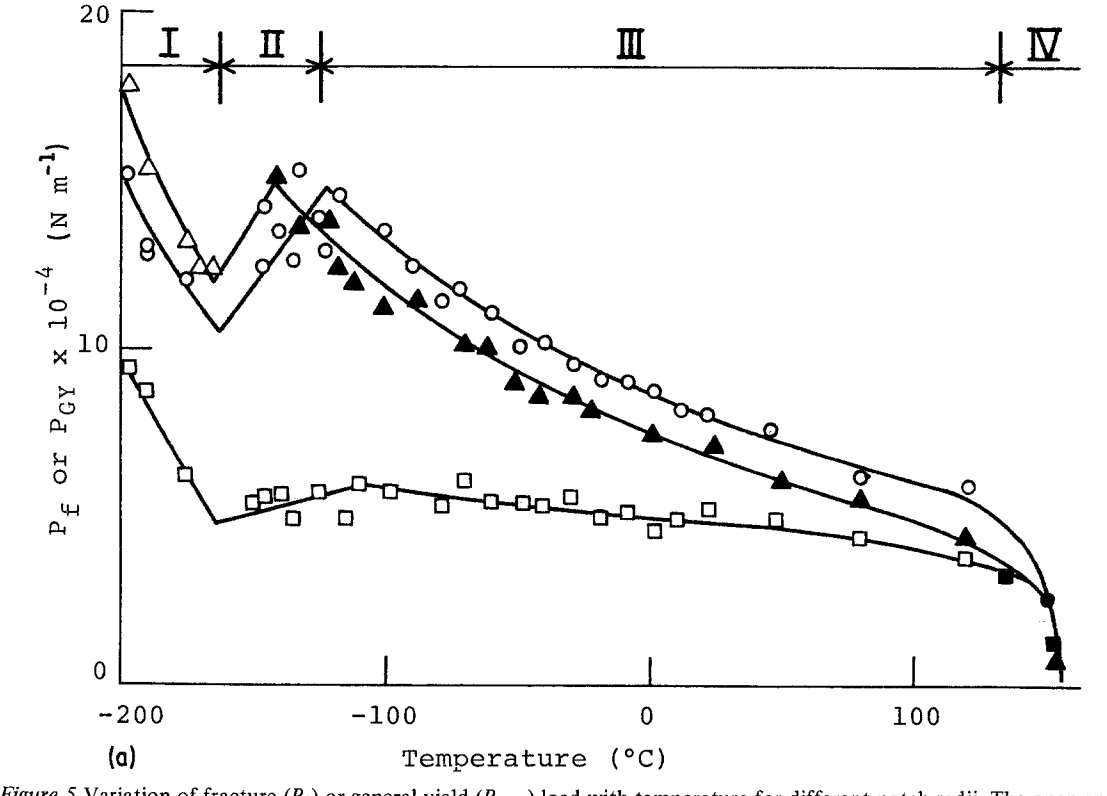

Figure 5 Variation of fracture (P_f) or general yield (P_{GY}) load with temperature for different notch radii. The open and solid marks correspond to fracture and general yielding, respectively. △ unnotched; ○ $\rho = 2$ mm; □ $\rho = 0.25$ mm. (a) PC; (b) PP.

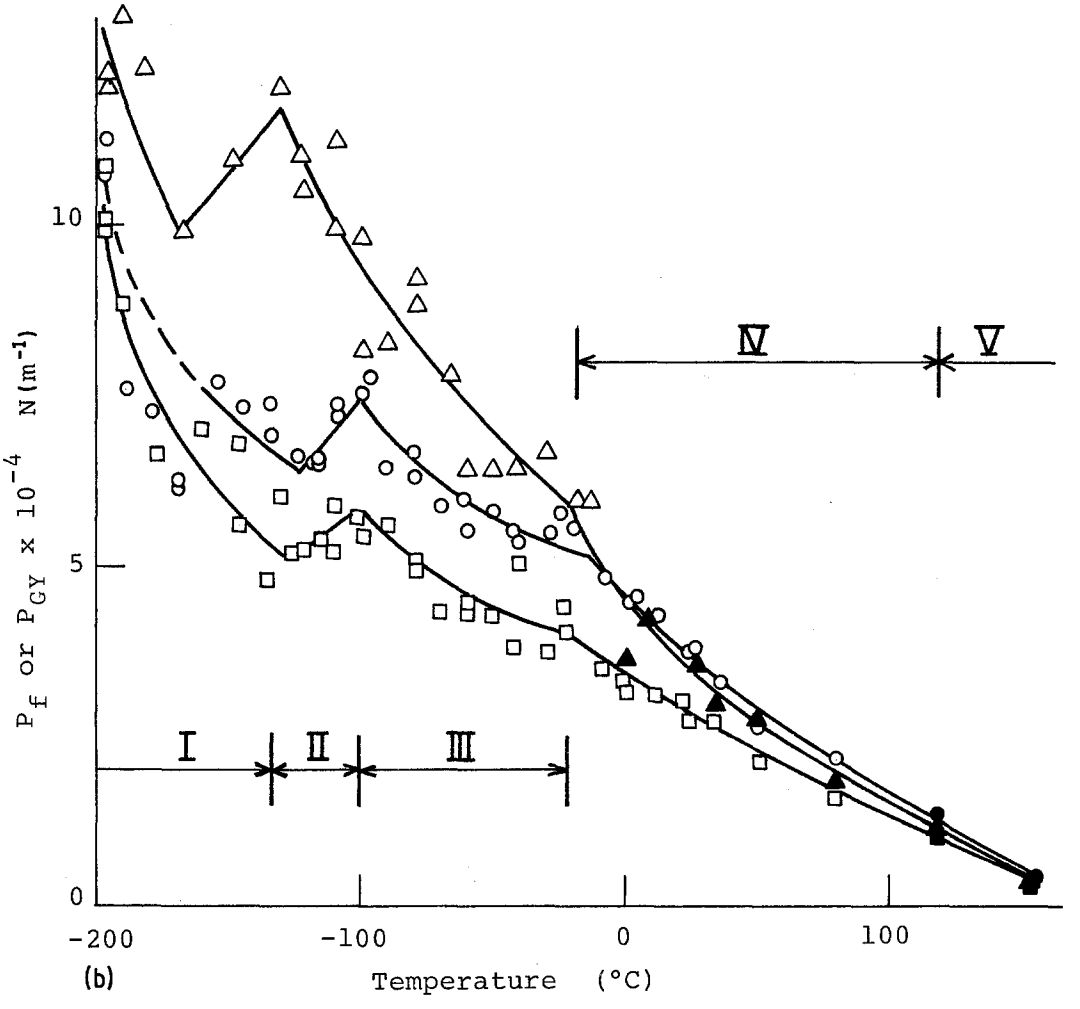

Figure 5 Continued

At first, we consider the characteristic regions for PC in the light of Fig. 6 where the fractographs near the notch root are shown.

(i) Region I: The stress required for craze initiation is probably smaller than the shear yield stress. Consequently, crazes initiate at the notch root before shear yielding occurs, and grow radially around the notch root. One of the crazes initiated opens to form a crack and the crack propagates slowly through the crazes to lead to a subsequent fast fracture. The fracture origin is adjacent to the notch root. The fracture surface consists of two regions, i.e. a mirror-like surface which includes the fracture origin and rough brittle fracture surface. The area of the mirror-like surface tends to increase with decreasing temperature.

This region is not observed in the tensile test of Brown and Imai [7] executed in N_2 gas.

(ii) Region II: Fracture stress decreases with decreasing temperature. As reflected in Fig. 6, shear bands initiate at the notch root before crazing occurs. Before the stress at the elastic–plastic interface becomes high enough to satisfy the condition for internal-craze nucleation, some crazes form at the notch root. Once the fracture nucleus, which is observed as a spot-like origin in the figure, forms among these crazes, it suddenly propagates in a brittle manner. Here, it is to be noted that the craze leading to fracture forms just below the notch root which already deforms plastically, whereas in Region II, it nucleates at an elastic state. According to [7], fracture in this region is caused by crazes which form due to an environmental attack of active gases. Further tests will be needed.

(iii) Region III: The final fracture starts at an elastic–plastic boundary where the stress reaches a critical level required for internal-craze nucleation. The details are reported in Fig. 7 of [2].

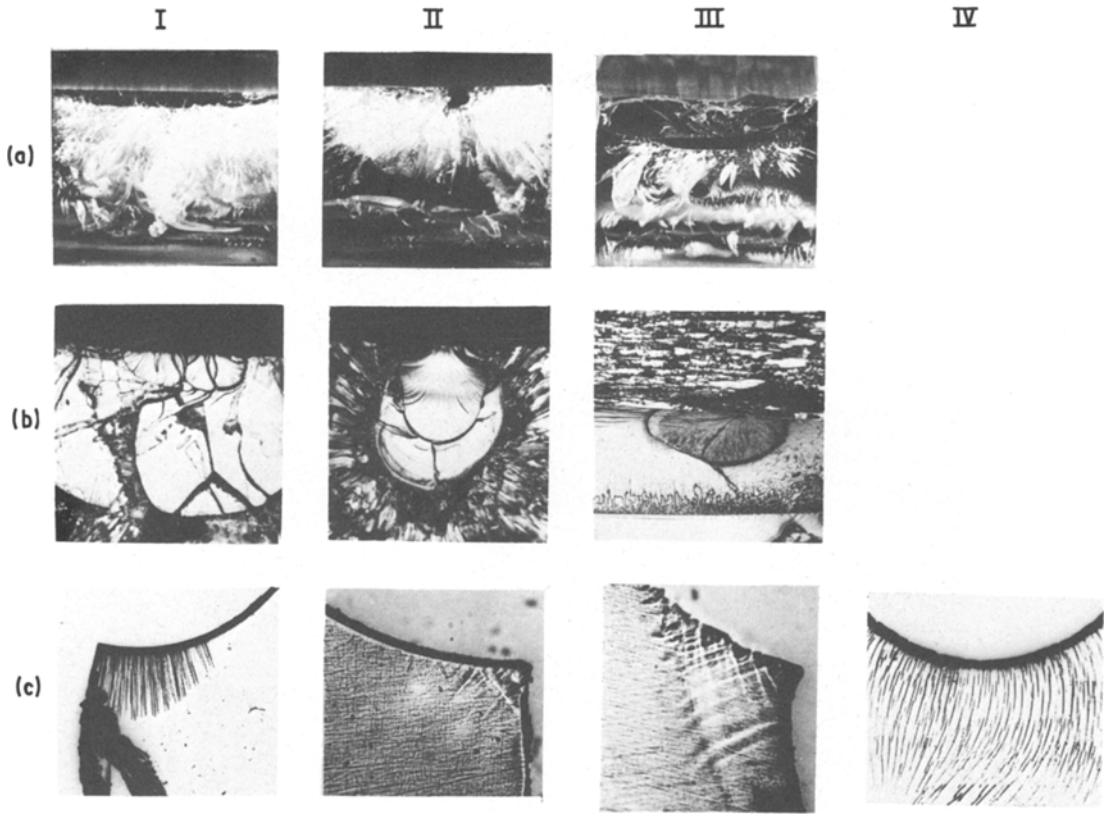

Figure 6 Fractographs at characteristic temperature regions in PC. The notch is placed at the upper side. The photographs (a), (b) and (c) are not always taken from the same specimen: (a) total fracture surface; (b) enlargement of fracture origin; (c) side view of notch part.

(iv) Region IV: General yielding occurs before fracture. The specimen deforms like rubber and the deformation is not always limited to the notch part. Surface curved crazes are observed around the notch.

As is evident from the above results, how crazes form around the notch seems to determine the characteristic fracture regions of PC. Slip-inducing fracture becomes dominant at relatively high temperatures, while craze-inducing fracture is valid at low temperatures.

Next, we consider the case of PP. The fracture behaviour is more complex than that of PC especially in Region I where the experimental data are considerably scattered. Following the definition denoted in Fig. 5, we describe the features in each region. The fractographs are shown in Fig. 7.

(i) Region I: A soon as the craze nucleates at the notch root, it propagates to cause a final brittle fracture. Few craze bands are observed around the notch root and the fracture origin is adjacent to the notch root. Only the brittle feature appears on the whole of the fracture surface.

(ii) Region II: Fracture load decreases with decreasing temperature. Crazes form at the notch root and grow inward. One of the crazes opens to propagate through the crazes over some distance to lead to a fast brittle fracture. Then, the fracture surface consists of two parts, i.e. a flat surface which denotes the slow crack growth through crazes and brittle fracture surface. The boundary which distinguishes the flat from the brittle surface is not always clear. The ratio of the flat area to the total fracture surface tends to increase with increasing temperature. The fracture process in this region may be similar to that in Region I of PC.

(iii) Region III: The fracture process is not so different from that in Region II. But the boundary between the flat and the brittle surfaces is more distinctive in this region than in Region II. As well as in Region II, the flat surface area increases with increasing temperature. In Regions I to III, the fracture origin is just below the notch root.

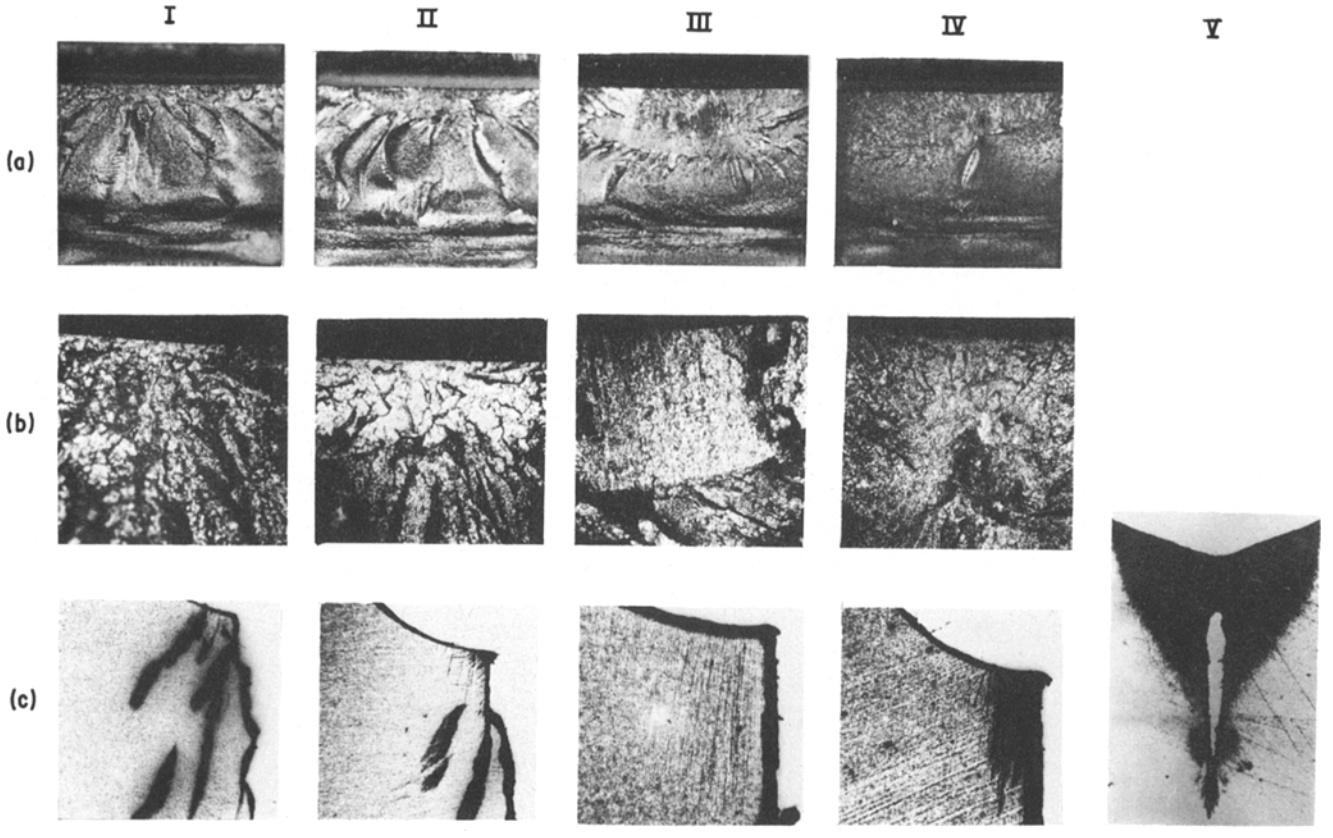

Figure 7 Fractographs at characteristic temperature regions in PP. The arrangement of the photographs is the same as Fig. 6.

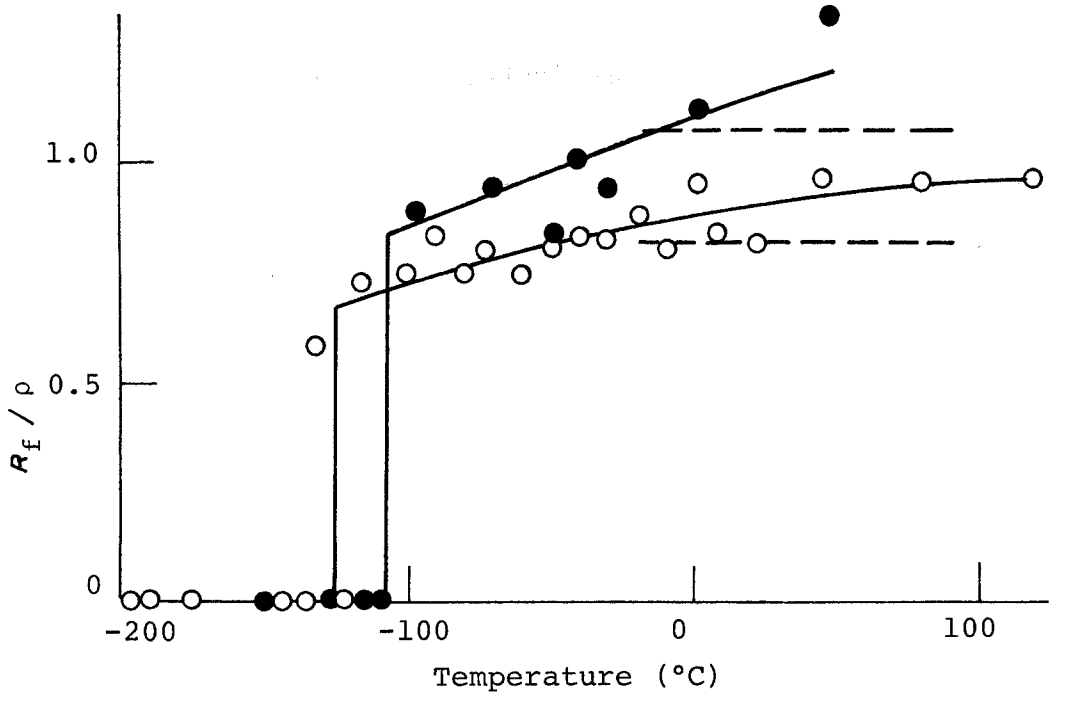

Figure 8 Effect of temperature on the position of fracture nucleus in PC. The solid and open circles denote the values for $\rho = 0.25$ and 2 mm, respectively. The dotted lines denote the previous results.

(iv) Region IV: The details of the fracture process are described in Section 4. The rate of increase in fracture load with temperature is steeper in Region IV than in Region III. The fracture surface is relatively smooth, and then is slightly different from those in the above regions.

(v) Region V: General yielding occurs before a complete fracture. Even if one of the intense craze bands opens to form a crack, it does not grow over the whole specimen since the large deformation at the notch root strengthens the material due to the orientation of polymer chains.

Roughly speaking, for PP, the features on the fracture surface are not so different over the entire ranges of temperatures tested, as compared with the results for PC. This may arise from the fact that the fracture of PP is mainly governed by the initiation and growth of crazes over all temperature ranges tested.

The results for both materials tested show that either of the plastic deformation modes, i.e. crazing and shearing, plays a governing role in the polymer brittle fracture.

6. Fracture criterion of PC

The fracture of PP is associated with the high density of crazes around the notch and the fracture origin is not always adjacent to the elastic–plastic interface. The high craze density may change the stress distribution due to the strain concentration. Unfortunately, the stress–strain relationship in the craze zone remains vague up to date. In this case, therefore, the slip line field analysis will lose its validity.

In this section, we discuss a fracture criterion for PC.

Measurements of the positions of fracture origin from the notch root, R_f, were made on PC samples tested at various temperatures. The ratios of R_f to the notch radius ρ, R_f/ρ, are plotted as a function of temperature in Fig. 8. The previous results are drawn by the dotted lines, which are comparable with the present data. The values of R_f/ρ are dependent on ρ at all temperatures in Region III, as noted in [2], and the ratio tends to slightly decrease with a decrease in temperature, whereas it suddenly drops down to zero at about $-110°C$. The sudden change of the ratio distinguishes Region III from Region II.

At first, we consider a fracture criterion in Region III. As inferred from Equation 1, a simple maximum principal stress theory that fracture occurs when the maximum stress reaches a critical level may not be valid, since R_f/ρ is dependent on ρ.

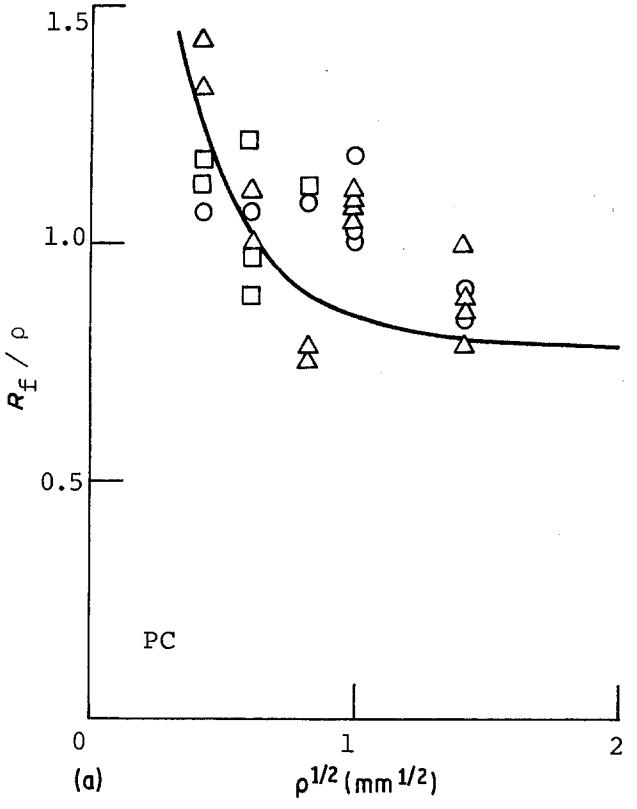

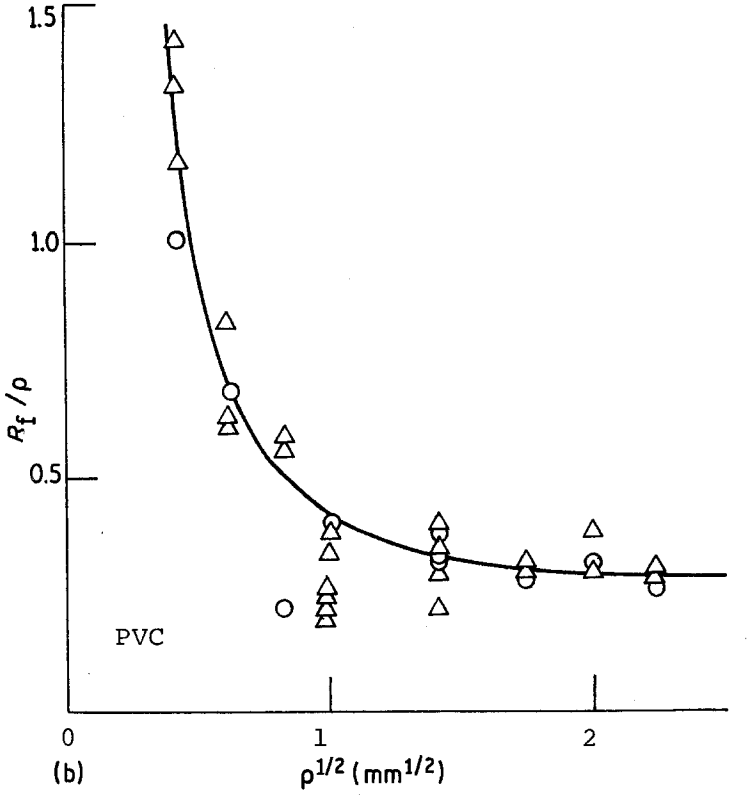

Figure 9 Variation of the position of fracture nucleus with notch radius in PC and PVC. (a) PC; (b) PVC.

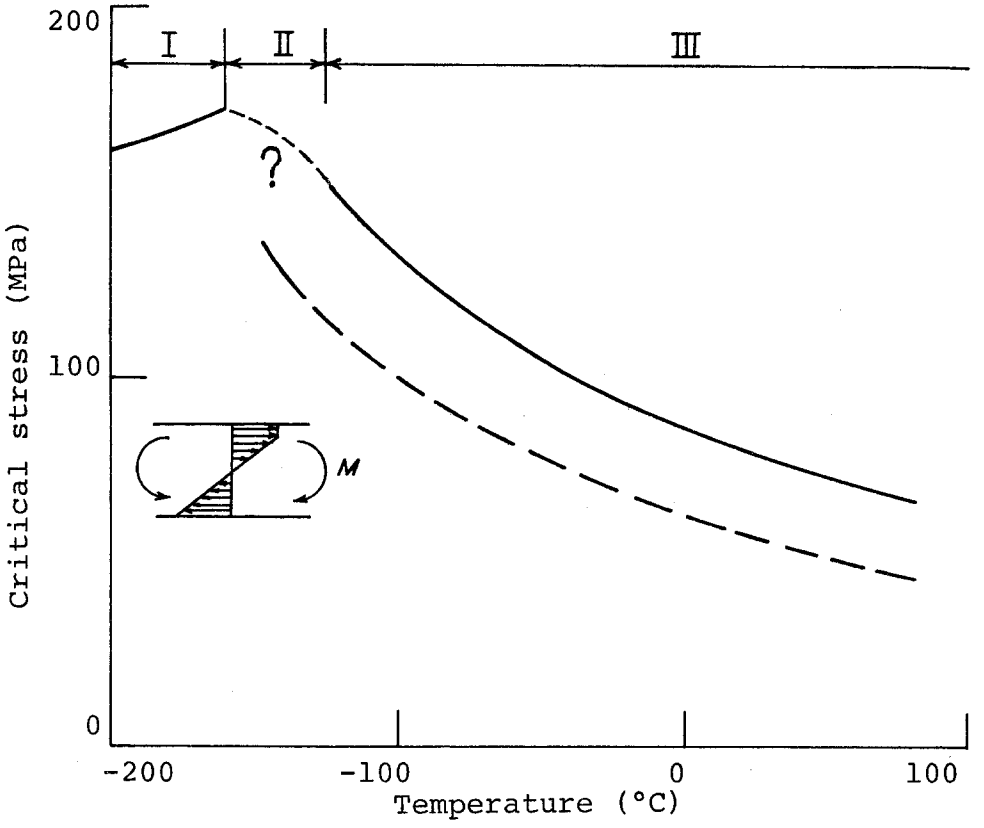

Figure 10 Temperature dependence of critical fracture stress determined from Equation 2. The solid and dashed curves show the fracture and yield stress, respectively.

For the purpose of confirming this prediction, the variations of R_f/ρ with ρ were measured in PC and PVC samples with different notch radii at room temperature. The fracture behaviour of PVC is shown to be similar to that of PC [2]. The results are indicated in Fig. 9 which also includes some data obtained from 4-point bending and tensile tests. Two important things are to be noted that (a) the position of the fracture nucleus is not so influenced by the testing method and (b) the ratio R_f/ρ considerably varies with the notch root radius. The probable reasons for these are due to the similarlity of the stresses in the plastically deformed region around the notch in spite of the difference of the testing method and a steep stress gradient at the notch tip. From this figure, we can confirm that the simple maximum stress theory for polymer brittle fracture loses its validity.

For explaining this, the previous paper [2] introduced the assumption that the stress σ_θ must exceed a critical value σ_f over at least an effective distance t_e to allow fracture initiation. According to this assumption, the fracture nucleus initation cannot occur when $\sigma_\theta = \sigma_f$ at the elastic–plastic boundary. If $\sigma_\theta = \sigma_f$ over t_e, a fracture nucleus will form. This concept was successfully applied to notch brittle fracture of mild steel as indicated by Tetelman *et al.* [6].

Based on this assumption, the condition for fracture nucleation is expressed from Equation 1 by

$$\sigma_f = \left[1 - \frac{1 - \sin\Phi}{1 + \sin\Phi}\left(1 + \frac{R_f - t_e}{\rho}\right)^{\xi}\right] C \cot\Phi \tag{2}$$

If the ratio R_f/ρ is set equal to δ in the case where $R_f \gg t_e$, i.e. very large ρ, Equation 2 reduces to

$$\frac{R_f - t_e}{\rho} = \delta \tag{3}$$

The solid lines in Fig. 9 show Equation 3 with $t_e = 90\,\mu m$ for PC and $T_e = 170\,\mu m$ for PVC. The values of t_e are chosen so that Equation 3 may fit the experimental data. Although the physical meaning of the effective distance t_e remains vague for amorphous polymers which may not have a macroscopic structural unit like a grain diameter

of steel and the applicability of Equation 1 to soft materials is somewhat questionable, Equation 3 becomes a useful criterion for notch brittle fracture at Region III in amorphous polymers.

The constants C and Φ can be determined from the general yield load for unnotched specimen and the intersection angle between slip bands. The value of Φ measured was about 10° that was nearly independent of temperature [2]. The critical stresses σ_f at temperatures in Region III are calculated using Equation 2 and the values of B, Φ and t_e. The variation of σ_f with temperature computed in this way is shown in Fig. 10 where $\Phi = 10°$ and $t_e = 90\mu m$. The calculated values of σ_f become independent of ρ, but are considerably sensitive to temperature. The dotted curve in the figure denotes the computed values of σ_θ at the notch root.

Next, Region I is considered. The yield stress is higher than the crazing stress, and then crazes initiate nearly in an elastic state. The plastic constraint is not required for craze initiation. Since the densely distributed crazes, as shown in Fig. 6, probably changes the elastic stress field, the calculation of the stresses around the notch based on the theory of elasticity may become meaningless. Then, the critical stress σ_f was estimated using the fracture data for unnotched specimens based on the assumptions that (a) the stress within the crazing layer is constant while the stress at the other section changes linearly as illustrated in Fig. 10 and (b) the depth of the layer varies linearly from 0 at −160° C to 1.5 mm at −197° C with decreasing temperature. The result calculated in this way is shown in Fig. 10. σ_f is nearly insensitive to temperature. Since the notched specimen fractures elastically with few crazes at −160° C where the transition from Region I to II occurs, the fracture stress can be also obtained from the result for notched specimen. The stress computed using a stress concentration factor of 1.2 for a $\rho = 2$ mm specimen was nearly equal to the value for unthe notched specimen. The stress computed using a stress concentration factor of 1.2 for a $\rho = 2$ mm denoting σ_θ at $r/\rho = 1$. This may show that the transition occurs at a temperature where the yield stress becomes equal to the crazing stress.

Finally, Region II which combines Region I and III is considered. Fracture starts at a spot-like origin just below the notch root which already plastically deforms. Hence, the stress σ_θ at the notch root which must be equal to $C \cot \Phi$ as predicted from Equation 1 will vary with temperature along the broad dotted line in Fig. 10. If so, the discontinuity of the fracture stress between Regions II and III is brought about at −120 or −110° C. The discontinuity may be caused by an environmental attack of nitrogen gas to the polymer, as indicated by Brown and Imai [7]. But the probable reason for this is not found in this paper. Future work will be needed.

7. Conclusion

The effect of temperature on the brittle fracture process of notched specimens of PC and PP was investigated in the wide ranges from −197° C to 150° C at 3-point bending test, and the slip line field analysis was used for discussing a fracture criterion. The results are summarized as follows:

1. The experimental slip line field at general yielding fairly agrees with the theoretical one which takes into account the effect of hydrostatic stress component on the yield condition. This may show that the slip line field analysis is successfully applied to soft materials like polymers.

2. There exist some characteristic temperature regions for brittle fracture. For PP, the initiation and extension of crazes govern the fracture over the whole temperature ranges tested. For PC, at relatively high temperatures, the internal craze away from the notch root which is nucleated by the stress increase due to the plastic constraint of shear bends becomes the fracture of origin, and at low temperatures, the surface crazes associated with or without slip bands at the notch root become a direct precursor of the fracture. At any rate, for both polymers used, how crazes initiate may determine the characteristic temperature region.

3. For PC, in the temperature Region III where shear bands govern the initiation of fracture, the ratio of the distance of the fracture origin to the notch radius is expressed as a function of the notch radius. According to the slip line field analysis, a simple maximum stress theory does not explain the present experimental result.

The fracture criteria in Region II for PC and in all regions for PP are not successfully explained in this paper. Further work will be required especially in connection with the effect of gas environment on the craze initiation at low temperatures using amorphous and crystalline polymers.

Acknowledgement

We are grateful to Mr Y. Kuroda and Mr K. Teguri for their technical assistance.

References

1. N. ISIKAWA, I. NARISAWA and H. OGAWA, *J. Polymer Sci.* **A-2 15** (1977) 1971.
2. M. KITAGAWA, *J. Mater. Sci.* **17** (1982) 2514.
3. A. S. TETELMAN and McEVILY, "Fracture of Structural Materials" (John Wiley & Sons, Inc., New York, 1967).
4. A. P. GREEN, *Quart. J. Mech. Appl. Math.* **6** (1953) 223.
5. A. MAKINOUCHI, *J. Jpn. Soc. Tech. Plasticity* **17** (1976) 140 (in Japanese).
6. T. R. WILSHAW, C. A. RAU and A. S. TETELMAN, *Int. J. Eng. Fract. Mech.* **1** (1986) 191.
7. N. BROWN and Y. IMAI, *J. Appl. Phys.* **46** (1975) 4130.

Received 4 March
and accepted 21 September 1983